Progress In Electromagnetics Research B, Vol. 40, 325–341, 2012

SOME NUMERICAL AND EXPERIMENTAL OBSERVATIONS ON THE GROWTH OF OSCILLATIONS IN AN X-BAND GUNN OSCILLATOR

B. C. Sarkar[1, *], C. Koley[1], A. K. Guin[1], and S. Sarkar[2]

[1]Physics Department, Burdwan University, Burdwan 713104, India

[2]Electronics Department, Burdwan Raj College, Burdwan 713104, India

Abstract—The dynamics of the onset of oscillations in a wave guide cavity based Gunn Oscillator (GO) has been critically examined through numerical simulations and experimental studies. The transition of the GO from a non-oscillatory to an oscillatory state and the same in the reverse direction occurs at different critical values of the dc bias voltage applied to the GO. In presence of a weak RF field in GO cavity, oscillations with broad band continuous spectrum and multiple discrete line spectrum are observed at the GO output for different values of dc bias below the above mentioned critical values. Analysing the numerically obtained time series data, chaos quantifiers have been obtained to prove the occurrence of the chaotic oscillations in the GO. Experimental results and observations of numerical simulation show good qualitative agreement.

1. INTRODUCTION

The physics of operation of a wave guide cavity based Gunn Oscillator (GO) has been studied at length during last fifty years since the invention of the Gunn diode in the early sixties of the last century [1–6]. A number of theoretical models for the GO have been proposed in the literature to explain the obtained experimental observations regarding the onset and the stabilization of oscillations in a GO [7–9]. It is established that when a Gunn diode is biased at a dc voltage above a threshold value, the negative differential resistance (NDR) of the diode compensates the resistive component of the cavity impedance and the system breaks into self oscillation at a frequency determined by the

Received 28 March 2012, Accepted 28 April 2012, Scheduled 7 May 2012

* Corresponding author: Bishnu Charan Sarkar (bcsarkar_phy@yahoo.co.in).

cavity and the device reactances [10]. In these studies the cavity is considered to be free from external RF field except those from thermal noise.

Several other works have also been reported in the literature describing and explaining the nonlinear dynamics of a GO [11, 12]. It is well known that bifurcation and chaos are observed in a GO under the influence of external periodic driving signals when the GO is operating in the normal active region [5, 15]. Some studies have considered the presence of microwave frequency ac signals with the dc and thus obtained spatiotemporal chaos in the oscillator [14, 15]. These studies are predominantly theoretical and concentrated on the physical aspects of Gunn Effect. Further, to the knowledge of the authors, the effect of gradual systematic increase of the dc bias in presence of RF field in the GO cavity was not considered.

The present work intends to revisit the problem of onset of oscillations in a GO when the oscillator cavity contains a weak external RF field and the dc bias voltage (V_B) is below the threshold value. The effect of the variation of frequency and power of the RF field present within the cavity on the dynamics of the GO under such conditions is also examined. It is shown by the numerical simulation and by experimental studies that the under biased GO (i.e., a GO having V_B less than the threshold dc value for NDR region of operation) exhibits different dynamical states. They are respectively non oscillatory, quasi periodic, chaotic and periodic oscillatory states depending upon the value of the dc bias.

The paper is organised in the following way. In Section 2, after brief description of the hardware structure of the GO, a circuit theoretic model of the system and differential equations describing the dynamics are given. The system equation can easily be identified as a modified Duffing oscillator equation with a term proportional to the cube of the damping term. The dynamics of such a system is potentially reach in nonlinear phenomenon (like chaos etc.) and well studied in the literature [13, 16–18]. However, the dynamics of a GO with variable dc bias can be studied by this equation after proper modelling of the practical situation. The effect of the variation of the GO is taken into account by considering the variation of some of the device parameters in the oscillator model. These parameters are dependent on resistance and reactance of the diode. Section 3 describes the results of numerical simulation. The obtained time series data sets are examined with the help of commercial Chaos Data Analyser (CDA) software for identification of different dynamical states of the system. Standard chaos quantifiers like maximal Lyapunov exponent (MLE) and correlation dimension (CD) are calculated. However no attempt

has been made to explain the route to chaos etc in this work. The obtained results of the hardware experiment are reported in Section 4. They confirm the occurrence of chaotic, quasi periodic and periodic states of the GO for different values of the applied dc voltage. The paper is concluded in Section 5 discussing the importance of the whole study.

2. CIRCUIT THEORETIC MODEL OF THE OSCILLATOR

From the knowledge of the operation of a Gunn diode, biased at the active region, it can be modelled by a parallel or series combination of two voltage dependent nonlinear circuit elements — one resistive and the other capacitive in nature. As the applied dc voltage across the diode crosses the threshold value it operates in NDR region and the value of this NDR is a function of the magnitude of V_B. Therefore, the relation between the incremental current (i) through the diode and the incremental voltage (v_r) across the diode is a nonlinear one. Considering the nonlinearity as cubic type, one writes it as

$$v_r = -\beta_1 i + \beta_3 i^3 \tag{1}$$

Here, β_1 and β_3 are the parameters taking care of linear and nonlinear dependence between the voltage and the current. Their magnitudes are determined by the value of the applied V_B. Above the threshold value β_1 is negative. The diode capacitance in the ac model is taken as voltage dependent due to the modification of the effective dielectric constant of the diode material in the presence of the negative charge in the active condition [8]. Thus one can write the instantaneous voltage (v_c) across the equivalent capacitor in terms of the instantaneous charge ($q = \int i \cdot dt$) as

$$v_c = -\alpha_1 q + \alpha_3 q^3 \tag{2}$$

Here α_1 and α_3 are the parameters taking care of linear and nonlinear components of diode capacitance. Thus the Gunn diode is replaced by a series combination of two nonlinear voltage sources v_r and v_c when an instantaneous current $i(= \frac{dq}{dt})$ passes through it. The wave guide type cavity is replaced by a series combination of inductor L, capacitor C and the resistor R. This R takes care of the cavity loss and the load resistor. Figure 1 shows the ac circuit theoretic model, of the GO. The voltage source v_s indicated in Figure 1 represents the presence of the external field within the cavity. It is replaced by a short circuit when there would be no external field present other than the noise voltage due to the finite temperature in the cavity.

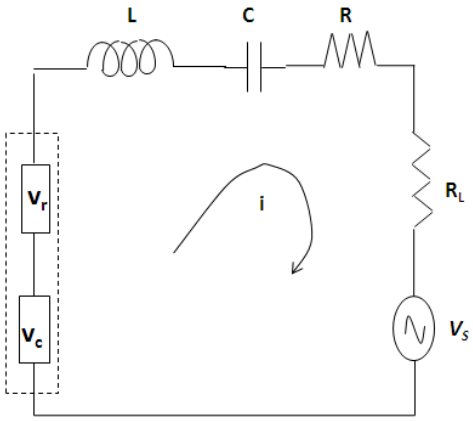

Figure 1. Series equivalent circuit of the Gunn Oscillator.

The differential equation describing the dynamics of the system is derived from the model depicted in Figure 1 applying the Kirchhoff's mesh law. The obtained equation is written as follows after some logical substitution and normalization [19]:

$$\frac{d^2q}{d\tau^2} = aq - bq^3 + c\frac{dq}{d\tau} - d\left(\frac{dq}{d\tau}\right)^3 + q_s\cos(\Omega\tau) \tag{3}$$

Here $\frac{dq}{dt} = i$ is the instantaneous circulating current and $\tau(=\omega_r t)$ is the normalized time. $\omega_r(=\frac{1}{\sqrt{LC}})$ represents the resonant frequency of the cavity. q_s and Ω are respectively the charge equivalent to the amplitude and the normalized angular frequency of the external field present within the cavity. The coefficients a, b, c and d are related with the resistive and the reactive parts of the device and the cavity impedances as follows:

$$a = \alpha_1 C - 1 \tag{4}$$

$$b = \alpha_3 C \tag{5}$$

$$c = \frac{\beta_1 - R - R_L}{\omega_r L} \tag{6}$$

$$d = \frac{\beta_3 \omega_r}{L} \tag{7}$$

It is evident the coefficients a, b, c and d are implicitly dependent on the magnitude of V_B through bias dependent parameters β_1, β_3, α_1 and α_3. Since α_1 and α_3 are related to the capacitive parameters, their values determines the oscillation frequency. As β_1 and β_3 are

related to the device resistance so they demand more attention in the analysis of onset of oscillation. Also the relative magnitude of β_3 is much less compared to β_1, hence the parameter d can be taken smaller than c. The effect of variation of the applied dc bias would be studied by considering the variation of c. Note that the increase in the value of V_B results in the decrease in the value of c [19].

3. NUMERICAL ANALYSIS

It is difficult, if not impossible, to get a general closed form solution of (3). So a numerical solution of it is obtained in the following way. We introduce a new state variable p and write:

$$\frac{dq}{d\tau} = p \tag{8}$$

$$\frac{dp}{d\tau} = aq - bq^3 + cp - dp^3 + q_s \cos(\Omega\tau) \tag{9}$$

Then, (8) and (9) are modelled using the MATLAB based Simulink software. This is shown in Figure 2. First we study the dynamics of the GO in the absence of any external RF field by

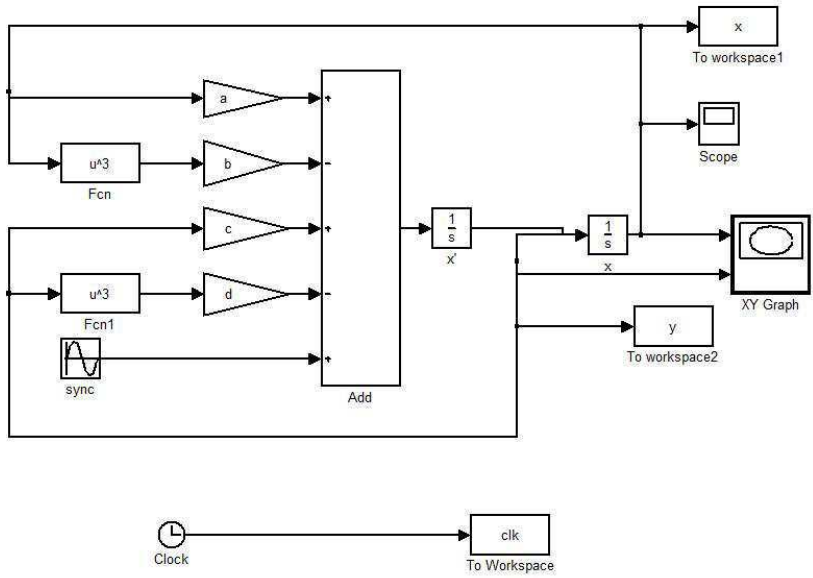

Figure 2. Simulink model of Gunn Oscillator in presence an external RF source.

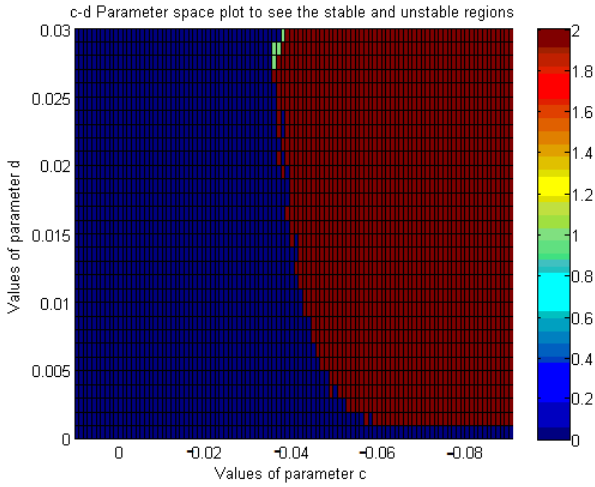

Figure 3. c-d parameter space plot to see non oscillatory (blue color) and stable oscillatory (red color) region of the free running Gunn Oscillator ($a = 1$, $b = 1$).

disconnecting the sinusoidal source from the Simulink model of GO. Considering $a = 1$ and $b = 1$, we take different pairs of values for c and d and perform the simulation to find the dynamical state of the system. The obtained state is either oscillatory or non-oscillatory in nature. Figure 3 shows the parameter space involving c and d resulting into these two states. Using Figure 3 the steady state values of q and p are obtained for a particular set of values of a, b, c and d. These values of q and p are taken as initial values for the next simulation with increased (decreased) value of c. We take $a = 1$, $b = 1$, $d = 0.015$ and examine the effect of the variation of c. As c decreases gradually from 0.06 the system begins to oscillate at $c = -0.06$. With these parameter values, the normalized frequency and amplitude of the free running GO are calculated as 1.27 and 2.0 respectively. Then, increasing the value of c from -0.06 the quenching of oscillation is obtained at $c = 0.01$. These two different values of indicate the occurrence of 'hysteresis' phenomenon in the onset and quenching of oscillation in a GO as a function of the dc bias voltage.

The effect of the external RF field is examined by considering the additional term $q_s \cos(\Omega\tau)$ in (9). With $a = 1$, $b = 1$, $d = 0.015$ as before, we take q_s and Ω as 0.15 and 1.27 respectively (This ensures the presence of a weak RF field of frequency close to the free running frequency of the GO in the cavity). Then we repeat the numerical

experiment of the bias variation by changing the parameter. From the evaluated time series data, instantaneous peak amplitudes of the oscillation have been obtained for a particular value of c and the same have been shown in Figure 4. The simulation has been repeated for different values of c. Figure 4 shows that the dynamics of the GO is considerably modified due to the presence of weak RF field in the cavity. Its transition from a non-oscillatory to an oscillatory mode is not abrupt as is obtained in the absence of RF field. With the variation of the value of c, chaotic and quasi periodic states are obtained in the GO dynamics before a stable oscillation is achieved. Results of numerical simulation with $c = -0.001$ are shown in Figure 5. The time variation of q and the phase space diagram using state variables q and p are shown in Figures 5(a) and 5(b) respectively. The variation of q with time is irregular in nature and the phase space plot is double scroll type. This indicates that the dynamics of the system is potentially chaotic. The frequency spectrum of q obtained by the First Fourier Transform of the time series data is Broad Band Continuous type shown in Figure 5(c). This is a signature of chaotic signal. Thus the state of oscillation is qualitatively recognized as chaotic. But for the quantification of chaos, different chaos quantifiers such as Maximal Lyapunov Exponent (MLE), Correlation Dimension (CD) etc. are to

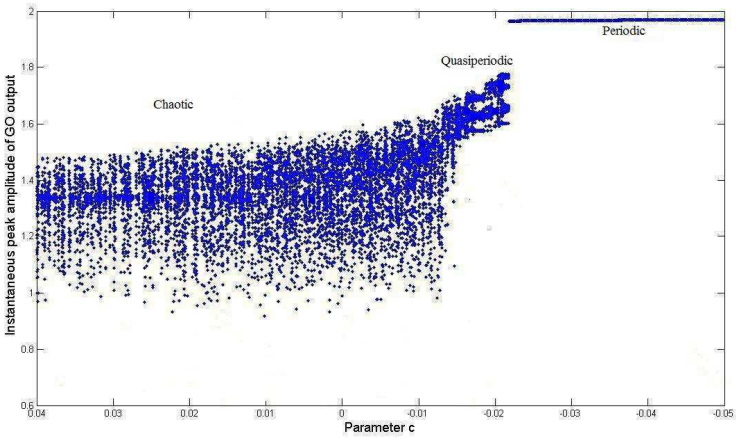

Figure 4. Variation of the instantaneous output peak amplitude of the Gunn Oscillator with the parameter c indicating chaotic, quasi periodic and stable periodic oscillatory states ($a = 1$, $b = 1$, $d = 0.015$, $q_s = 0.15$, $\Omega = 1.27$).

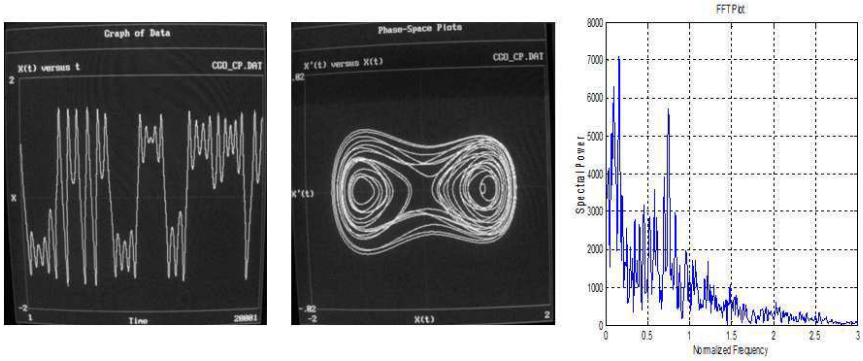

(a) (b) (c)

Figure 5. (a) Time domain, (b) phase space, (c) frequency spectrum of the GO output ($a = 1$, $b = 1$, $c = -0.001$, $d = 0.015$, $q_s = 0.15$ and $\Omega = 1.27$).

be evaluated. The Lyapunov exponent is a measure of the rate at which nearby trajectories in phase space diverges. In general there are as many exponents as there are dynamical equations and for chaotic orbits there must have at least one positive Lyapunov exponent [20, 21] where as for periodic orbits, all Lyapunov exponents are negative. Correlation dimension is another measure of the complexity of the system [22, 23]. It takes into account of the density of points of the attractor. While the computation of MLE is based on the behavior of the system in time domain, that of CD focus on the geometric structure of the attractor in the state space. A non integer value of the CD would indicate the attractor to be strange and thus the dynamics as chaotic. We have evaluated MLE and CD from the time series data as obtained from the numerical experiment and using the CDA by J. C. Sprott [24]. Figures 6(a) and 6(b) show respectively the variation of the evaluated MLE and CD for different values of the parameter c. Positive values of MLE and non-integer values of CD have been obtained for a range of values of c. Specifically, the values of MLE obtained for the given range of c are in the range 0 to 0.013 and those of CD in the range 1.1 to 1.9. Small but positive values of MLE indicate that the dynamics is chaotic and this observation is further supported by non-integral values of CD. However, the deterministic chaos thus obtained is low dimensional and controllable [21–23, 25, 26]. We have also obtained Return Map of the time series data using CDA [24] as two-dimensional phase-space plot generally will not distinguish between random and chaotic data. The return map is shown in Figure 6(c). It depicts the value of q at the

time when p equals a constant versus the value of q at the previous time at which p equalled the same constant. The obtained return map indicates the chaotic dynamics of the system for the selected set of the time series data.

In order to study how the frequency of the weak RF field affects the dynamics of the under biased GO, numerical simulation has been done by taking the values of the parameters a, b and d as before with $c = -0.001$, and then varying Ω. Figure 7 shows variation of

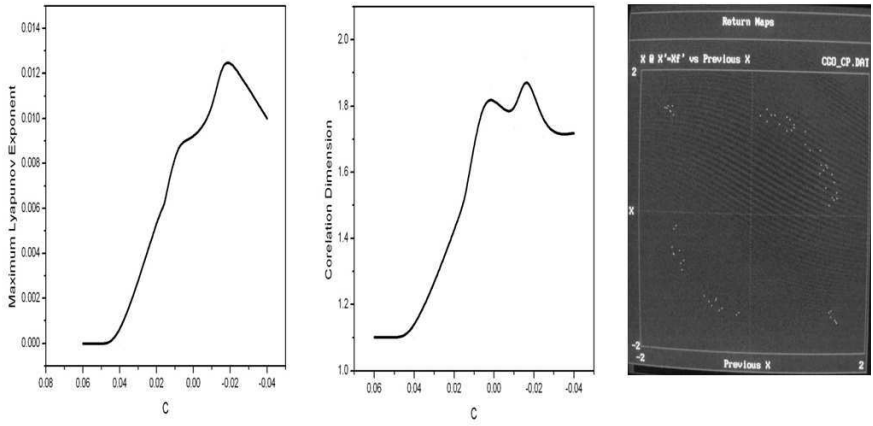

Figure 6. Variation of (a) MLE, (b) CD with the parameter c, (c) return map of the time series data ($a = 1$, $b = 1$, $c = -0.001$, $d = 0.015$, $q_s = 0.15$ and $\Omega = 1.27$).

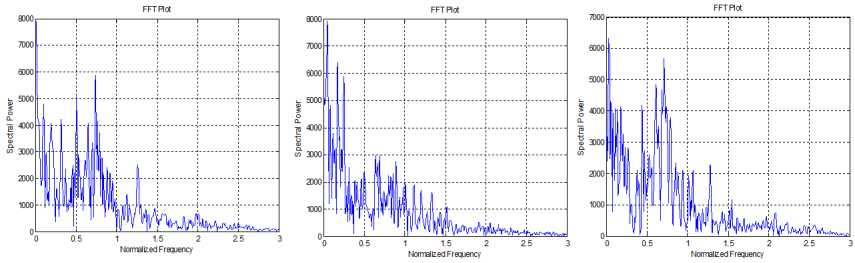

Figure 7. Frequency spectra of the GO output (a) $\Omega = 1.256$, (b) $\Omega = 1.269$, (c) $\Omega = 1.279$ ($a = 1$, $b = 1$, $c = -0.001$, $d = 0.015$ and $q_s = 0.15$).

the frequency spectrum of the GO for different values of Ω. It has been observed as the frequency of the RF field is close to the free running frequency of the GO, the chaotic behavior in the dynamics of the oscillator is pronounced. From the time series data, two chaos quantifiers MLE and CD respectively are evaluated with the help of CDA [21] and their variations with Ω are shown in Figures 8(a) and 8(b) respectively. The obtained values of MLE and CD are within the ranges 0.009 to 0.013 and 1.5 to 1.9 respectively. Thus the chaotic dynamics of the system is low dimensional and controllable in nature.

4. EXPERIMENTAL STUDIES

Figure 9 shows the block diagram of the experimental set up. The actual hardware arrangement shown in Figure 10 is designed using the

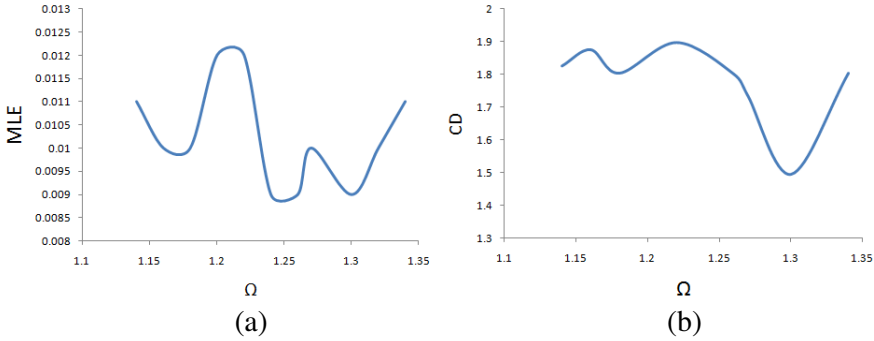

Figure 8. The variation of (a) MLE, (b) CD with the normalized frequency (Ω) of the external RF field ($a = 1$, $b = 1$, $c = 0.01$, $d = 0.015$ and $q_s = 0.15$.)

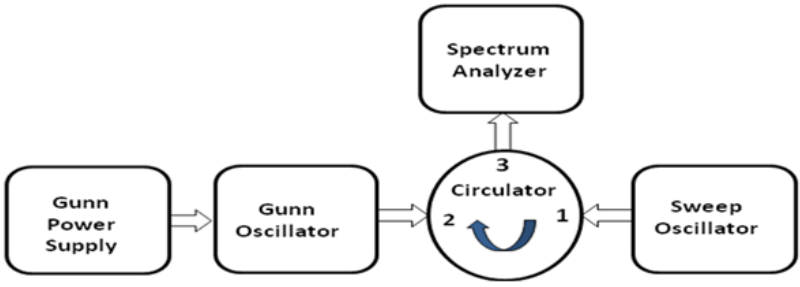

Figure 9. Block diagram of the experimental set up.

components like a waveguide type Gunn Oscillator (Model. No. X2152, Serial No. 1031), a Gunn power supply (Model. No. NV101), a Microwave signal source (HP-8350B, 8–20 GHz) and a Circulator (Model. No. XC621, Serial No. 439). A Spectrum Analyser (SA) (Rohde and Schwarz, 9 kHz–18 GHz) is used to observe the output spectral characteristics.

The first part of the experiment is performed in the free running mode keeping the micrometer screw attached to the oscillator cavity in a suitable location. Then V_B applied to the Gunn diode is slowly increased and discrete line spectrum is observed in the SA at bias V_{BCi}, indicating the growth of sinusoidal oscillation at the GO output. A further increase of V_B results in the increase in the GO output power (P_o) and a slight change in the oscillation frequency (f_o). Then V_B is slowly decreased and the GO remains in the oscillatory state up to a bias voltage V_{BCd} which is less than the voltage required (V_{BCi}) for the growth of oscillation in the increasing mode. Table 1

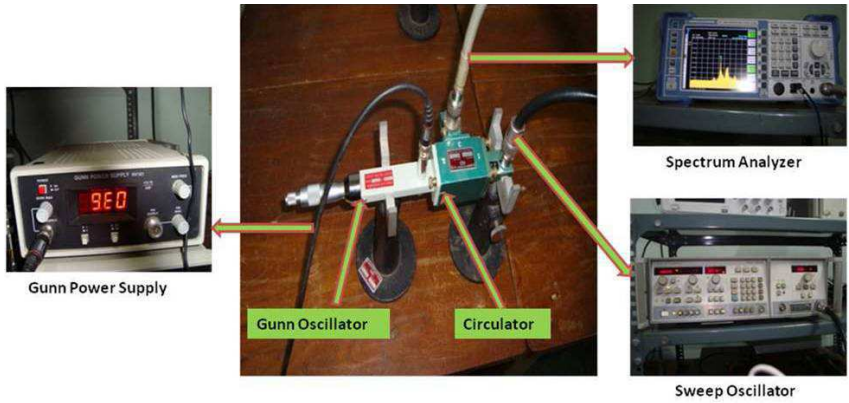

Figure 10. Hardware arrangement of the experimental set up.

Table 1. Experimentally obtained values of the GO dc bias required for the onset and quenching of oscillations.

Micrometer screw reading (mm)	v_{BCi} **(volts)**	**Oscillation frequency (GHz)**	**Output power (dBm)**	v_{BCd} **(volts)**
9.0	5.61	9.985	11.54	5.13
11.0	7.02	9.547	10.80	5.64
13.0	7.50	9.178	9.58	6.17

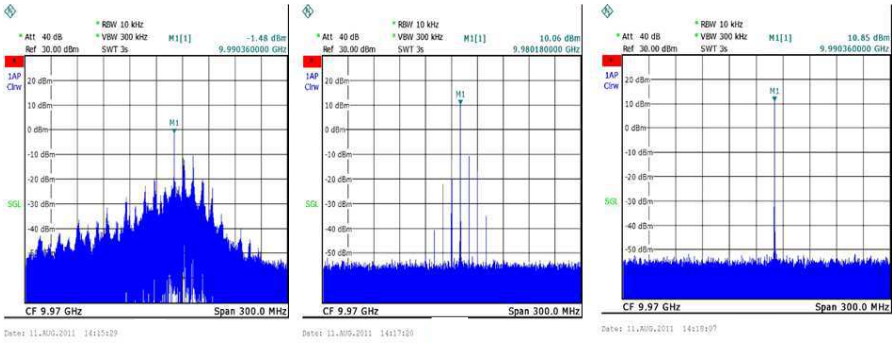

(a) (b) (c)

Figure 11. Experimentally obtained output spectrum of the under-biased GO in presence of an external RF signal having frequency 9.99 GHz and power −10 dBm. (a) V_B = 4.75 Volt (chaotic), (b) V_B = 5.26 Volts (quasi periodic), (c) V_B = 6.0 Volts (periodic).

represents experimentally obtained results for three different positions of the micrometer screw of the GO.

In the second part of the experiment, keeping the cavity length at a particular value (9 mm), an external RF signal having power ($P_S = -10$ dBm) which is considerably less than P_o (11.54 dBm) and frequency (f_{RF}) nearly equal to f_0 (= 9.99 GHz) of the GO is injected into the oscillator cavity. In this condition V_B is slowly increased. It is observed before the system is reached into the stable oscillating state; it passes through several complicated states such as Broad Band Continuous Spectra (BBCS), multiple discrete components. Afore mentioned states are equivalent to well known chaotic state and quasi-periodic state of GO oscillation. In the decreasing condition of the bias voltage, the oscillator transits from the stable oscillating state to no oscillating state through quasi-periodic and chaotic states again. However, these intermediate states occur at different values of V_B in this condition. Figures 11 show output spectrum at the GO in the increasing mode for three different values of V_B. They specify three different dynamical states (chaotic, quasi periodic and periodic) of the oscillator. The experiment is repeated by varying the power of the external RF signal and the obtained observations are summarised in Table 2.

In the third part of the experiment, V_B of the GO is kept fixed at 5.0 volts and f_{RF} is varied. It has been observed as f_{RF} changes towards the free running frequency of the GO; its output spectrum becomes chaotic. The obtained experimental observations are shown

Table 2. Experimental observations on the nature of the GO output spectrum for different values of the GO dc bias with a fixed power injected field in the GO cavity.

P_s **(dBm)**	V_B **(Volts)**	**Nature of the output spectrum of the GO**
−20	3.2	Non Oscillatory
	3.34	BBCS having peak power ($P_{\text{peak}} = -30$ dBm) 10 dBm Bandwidth (BW = 80 MHz)
	3.42	BBCS having $P_{\text{peak}} = -40$ dBm and BW = 60 MHz
	3.5	BBCS having $P_{\text{peak}} = -45$ dBm and BW = 50 MHz
	5.4	Quasi-Periodic having components 9.975 GHz (−45 dBm), 9.98 GHz (−15 dBm), 9.985 GHz (10.31 dBm), 9.90 GHz (−15 dBm), 9.95 GHz (−48 dBm)
	5.92	Periodic having frequency 9.99 GHz and power 10.76 dBm
−10	3.3	Non Oscillatory
	3.9	BBCS having peak power ($P_{\text{peak}} = -30$ dBm) BW = 90 MHz
	4.1	BBCS having $P_{\text{peak}} = -25$ dBm and BW = 90 MHz
	4.75	BBCS having $P_{\text{peak}} = -22$ dBm and BW = 120 MHz
	5.0	BBCS having $P_{\text{peak}} = -20$ dBm and BW = 100 MHz
	5.26	Quasi-Periodic having components 9.95 GHz (−40 dBm), 9.96 GHz (−30 dBm), 9.97 GHz (−20 dBm), 9.98 GHz (10.06 dBm), 9.99 GHz (−10 dBm), 10.0 GHz (−15 dBm),10.01 GHz (−35 dBm)
	6	Periodic having frequency 9.99 GHz and power 10.85 dBm

in Figure 12 for three different values of f_{RF}. They indicate the average power and bandwidth of the chaotic spectrum increases as f_{RF} becomes close to f_0. It has to be mentioned here that the generation of chaotic oscillations at the GO output is very much predictable for a particular arrangement of the GO circuit. The dc bias has to be adjusted slightly below the threshold bias required for the periodic oscillations and injected RF field frequency should be around resonant frequency of the cavity. The system can be used as a generator of robust deterministic chaos of low average power at the frequency range 9 GHz to 10 GHz. In the literature, one can find microwave frequency chaos generators using different forms of active circuits like colpitts oscillators, CMOS structure, phase locked loop etc. [27–31]. The quantification of the experimentally generated chaos in the GO based circuit could not be done here because of the non availability

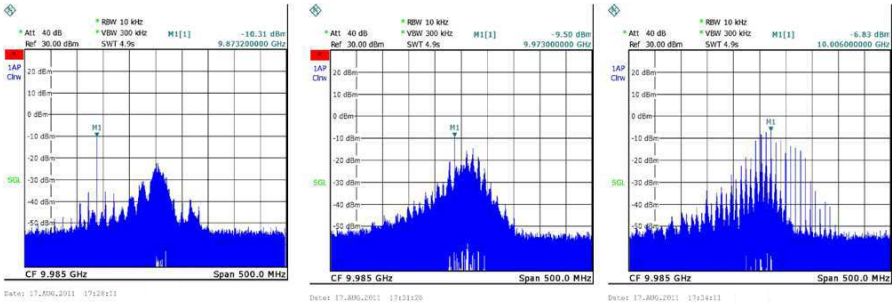

(a) (b) (c)

Figure 12. Experimentally obtained output spectrum of the under-biased GO ($V_B = 4.50$ Volts) in presence of an external RF signal having power -10 dBm. (a) $f_{\mathrm{RF}} = 9.88$ GHz, (b) $f_{\mathrm{RF}} = 9.98$ GHz, (c) $f_{\mathrm{RF}} = 10.06$ GHz.

of the time domain instruments (like X-band real time oscilloscope) in the authors laboratory.

5. CONCLUSION

The paper describes some new observations on the onset of oscillations in an X-Band GO. The presence of a weak RF field in the oscillator cavity is found to considerably modify the dynamics of the GO. In the absence of such field the dc bias of the GO is slowly varied from a low value and after a threshold value of the bias voltage the GO suddenly enters into the oscillatory state. However, with the decrease in the dc bias voltage the oscillation stops at some other lower value of bias. This asymmetry in dc bias voltage required for inducing and quenching of oscillations has importance from the nonlinear analytical point of view. In the presence of weak external RF field in the cavity the same experimental study indicates the occurrence of several dynamical states in the system like chaotic, quasi periodic and periodic oscillatory state for different value of bias voltage. The frequency and the power of the RF field are found to have pronounced effect on the details of the above mentioned dynamical features. With the help of a suitable circuit theoretic model of the GO, the whole observation has been numerically simulated. The process of dc bias variation is modelled by the variation of concerned system parameters. The simulation results qualitatively agree with the experimental results. Further, the numerical time series data are analyzed with the help of commercial CDA software to obtain common chaos quantifiers like MLE and CD. The obtained values of

these parameters confirm the chaotic dynamics of the GO. This study reported here additionally suggests a convenient method of generation of chaotic oscillation in an X-Band GO. The applied dc bias voltage below the threshold value and the external RF field to be applied in GO cavity could be the suitable control parameters of such chaos generator. This said system would have potential application in microwave chaotic communications.

ACKNOWLEDGMENT

Authors acknowledge partial financial assistance from DAE, BRNS (India) and DST (India) through sponsored research projects in carrying out the work.

REFERENCES

1. Kurokawa, K., "Injection locking of microwave solid state oscillator," *Proc. IEEE*, Vol. 61, 1386–1410, 1973.
2. Ito, Y., et al., "Cavity stabilized X-band Gunn Oscillator," *IEEE Transactions on Microwave Theory and Techniques*, Vol. 18, 870–897, 1970.
3. Holtzman, E. L. and R. S. Robertson, *Solid State Microwave Power Oscillator Design*, Chapters 2, 4 and 7, Artech House, Norwood, MA, 1992.
4. Solano, M. A., J. S. Ipina, J. M. Zamanillo, and C. P. Vega, "X-band Gunn diode oscillator for a multiple frequency continuous-wave radar for educational purposes," *IEEE Transactions on Education*, Vol. 45, 316–322, 2002.
5. Chakravorty, J., T. Banerjee, R. Ghatak, A. Bose, and B. C. Sarkar, "Generating chaos in injection-synchronized Gunn Oscillator: An experimental approach," *IETE Journal of Research*, Vol. 55, 106–111, 2009.
6. Ko, D. S., S. J. Lee, T. J. Baek, S. G. Choi, M. Han, H. C. Park, J. K. Rhee, J. H. Jung, and Y. W. Park, "New tuning method for 94 GHz waveguide voltage controlled oscillator," *IEEE Microwave and Wireless Components Letters*, Vol. 21, No. 3, Mar. 2011.
7. Kao, C. H. and L. W. Chen, "A hydrodynamic equivalent circuit model for the Gunn diode," *Solid-State Electronics*, Vol. 46, 915–923, 2002.
8. Pence, I. W. and P. J. Khan, "Broad band equivalent circuit determination of Gunn diodes," *IEEE Transactions on Microwave Theory and Techniques*, Vol. 18, No. 11, Nov. 1970.

9. Shalatonin, V., "Modeling of the nonlinear dynamics in a Gunn chaos oscillator," *18th Int. Crimean Conference in Microwave and Telecommunication Technology*, Sevatopol, Crimea, Ukraine, Sep. 8–12, 2008.
10. Hakki, B. W., "Amplification in two valley semiconductors," *J. Applied Physics*, Vol. 38, No. 2, 808–818, Feb. 1967.
11. Shiau, Y. H., "Stochastic resonance in the Gunn effect," *Physics Rev. B*, Vol. 60, No. 23, 15534–15537.
12. Mosekilde, E., et al., "Phase diagram for periodically driven Gunn diode," *Physica D*, Vol. 66, 143–153, 1993.
13. Lakshmanan, M. and S. Rajsekar, *Non Linear Dynamics, Integrability, Chaos and Patterns*, Springer, 2003.
14. Shiau, Y. H. and Y. C. Cheng, "Hybrid electric field domains leading to spatiotemporal chaos in N-GaAs," *Physical Rev. B*, Vol. 56, No. 15, 9247–9250, Oct. 1997.
15. Mosekilde, E., et al., "Mode locking and spatio-temporal chaos in periodically driven Gunn diode," *Physical Rev. B*, Vol. 41, 2298–2306, 1990.
16. Kao, Y. H., J. C. Huang, and Y. S. Gou, "Routes to chaos in duffing oscillator with one potential well," *IEEE International Symposium*, Vol. 1, 265–268, 1988.
17. Novak, S. and R. G. Frehlich, "Transition to chaos in the duffing oscillator," *Phys. Rev. A*, Vol. 26, 3660–3663, 1982.
18. Musielak, D. E., Z. E. Musielak, and J. W. Banner, "Chaos and route to chaos in coupled duffing oscillators with multiple degree of freedom," *Science Direct*, Vol. 24, 907–922, 2005.
19. Sarkar, B. C., D. Sarkar, S. Sarkar, and J. Chakraborty, "Studies on the dynamics of bilaterally coupled X-band Gunn oscillators," *Progress In Electromagnetics Research B*, Vol. 32, 149–167, 2011.
20. Jordan, D. W. and P. Smith, *Nonlinear Ordinary Differential Equations; An Introduction for Scientists and Engineers*, 4th Edition, Oxford University Press, 2009.
21. Hilborn, R. C., *Chaos and Non Linear Dynamics*, Oxford University Press, 2000.
22. Sprott, J. C., *Chaos and Time Series Analysis*, Oxford University Press, 2003.
23. Strogatz, S. H., *Nonlinear Dynamics and Chaos*, West View Press, 2007.
24. Sprott, J. C., *Chaos Data Analyzer Package*, Web address: http://sprott.physics.wisc.edu/cda.htm.

25. Ram, R. J., R. Sporer, H.-R. Blank, and R. A. York, "Chaotic dynamics in coupled microwave oscillators," *IEEE Transactions on Microwave Theory and Techniques*, Vol. 48, No. 11, 1909–1916, 2000.
26. Bulashenko, O. M., M. J. Garcia, and L. L. Bonilla, "Chaotic dynamics of electric-field domains in periodically driven superlattices," *Physical Rev. B*, Vol. 53, No. 15, 10008–10018, 1996.
27. Shi, Z. G. and L. X. Ran, "Microwave chaotic Colpitts oscillator: Design, implementation and applications," *Journal of Electromagnetic Waves and Applications*, Vol. 20, No. 10, 1335–1349, 2006.
28. Stefanidis, V., O. Tsakiridis, E. Zervas, and J. Stonham, "Design of a microwave chaotic oscillator using symmetric active load," *Latest Trends on Circuit*, 2010.
29. Jiang, T., S. Qiao, Z.-G. Shi, L. Peng, J. Huangfu, W.-Z. Cui, W. Ma, and L.-X. Ran, "Simulation and experimental evaluation of the radar signal performance of chaotic signals generated from a microwave Colpitts oscillator," *Progress In Electromagnetics Research*, Vol. 90, 15–30, 2009.
30. Nikishov, A. Y., "Generation of the microwave chaotic oscillations by CMOS structure," *PIERS Proceedings*, 457–461, Moscow, Russia, Aug. 18–21, 2009.
31. Dmitriev, A. S., A. V. Kletsov, and L. V. Kuzmin, "Experimental generation of chaotic oscillations in microwave band by phase-locked loop," *PIERS Proceedings*, 1498–1502, Moscow, Russia, Aug. 18–21, 2009.